

Copper(II) complexes of mono- and di-nucleating hexamines †

Paul V. Bernhardt* and Elizabeth J. Hayes

Department of Chemistry, University of Queensland, Brisbane, 4072, Australia

The potentially hexadentate polyamines *N,N,N',N'*-tetrakis(2-aminoethyl)ethane-1,2-diamine (L^1) and the octamethylated analogue *N,N,N',N'*-tetrakis(2-dimethylaminoethyl)ethane-1,2-diamine (L^2) have been complexed with copper(II) and the crystal structures of their complexes determined. A trigonal-bipyramidal co-ordination geometry for $[Cu(HL^1)][ClO_4]_3$ was found where one aminoethyl arm is not co-ordinated. By contrast, a dinuclear structure of formula $[(H_2O)Cu(L^2)Cu(OH)]^{3+}$ was determined for the *N*-methylated analogue, where the hexamine acts as a bridging ligand between the two square-pyramidal metal centres. Electronic and EPR spectroscopy are both consistent with these structures being maintained in solution.

The branched hexamine *N,N,N',N'*-tetrakis(2-aminoethyl)ethane-1,2-diamine (L^1) was first synthesized more than 45 years ago¹ but surprisingly few studies of its co-ordination chemistry have appeared subsequently,^{2,3} and structural reports of free L^1 (ref. 4) or its complexes^{5,6} are few. This is remarkable since the similarity between L^1 and the ubiquitous carboxylate analogue ethylenedinitrilotetraacetate (edta) is obvious. The hexamine L^1 is quite flexible and may adopt a number of conformations when co-ordinated. If less than six N-donors are bound to one metal then co-ordination modes reminiscent of well known polyamine relatives such as tren [tris(2-aminoethyl)amine], trien [*N,N'*-bis(2'-aminoethyl)ethane-1,2-diamine] and dien [bis(2-aminoethyl)amine] become possible. Some of these binding modes are illustrated in Fig. 1.

In an early study⁷ the complex-formation constants of L^1 with several divalent metal ions were determined by potentiometric titration. It was noted that some metal ions, including Cu^{II} , did not bind all six N-donors, but preferred pentadentate co-ordination. A structure similar to that shown in Fig. 1 (ii) was proposed for $[Cu(HL^1)]^{3+}$ to account for the titration data. Of particular interest to us is the potential for L^1 to act as a dinucleating ligand in conformations such as that shown in Fig. 1 (iv). This type of co-ordination has indeed been identified with metal ions such as Pt^{II} and Pd^{II} where the preference for square-planar co-ordination prohibits the ligand from binding to more than three co-ordination sites on the one metal ion.^{8,9}

We have attempted to modulate the preference for mono- or di-nucleating co-ordination modes by modification of the parent L^1 . *N*-Methylation is known to inhibit the co-ordinating ability of primary and secondary amines, primarily as a result of an increase in steric crowding. In tertiary polyamines these steric effects become so severe that co-ordination by more than about four N-donors to the same metal ion is rare. Indeed it is noteworthy that there are no known examples of six tertiary amines binding to the same metal ion. Therefore, the potentially hexadentate tertiary hexamine *N,N,N',N'*-tetrakis(2-dimethylaminoethyl)ethane-1,2-diamine (L^2) can be expected to favour dinuclear co-ordination modes in order to relieve non-bonded repulsion of the methylated N-donors. There is one report concerning L^2 ,¹⁰ but no details of its synthetic or spectroscopic characterisation were given. In addition, its co-ordination chemistry has remained unexplored. To this end, we have synthesized and characterised the copper(II) complexes of L^1 and its octamethylated analogue L^2 . As we will demonstrate, the effect of *N*-methylation going from L^1 to L^2 has a marked influence on the co-ordinating ability of these potentially hexadentate ligands.

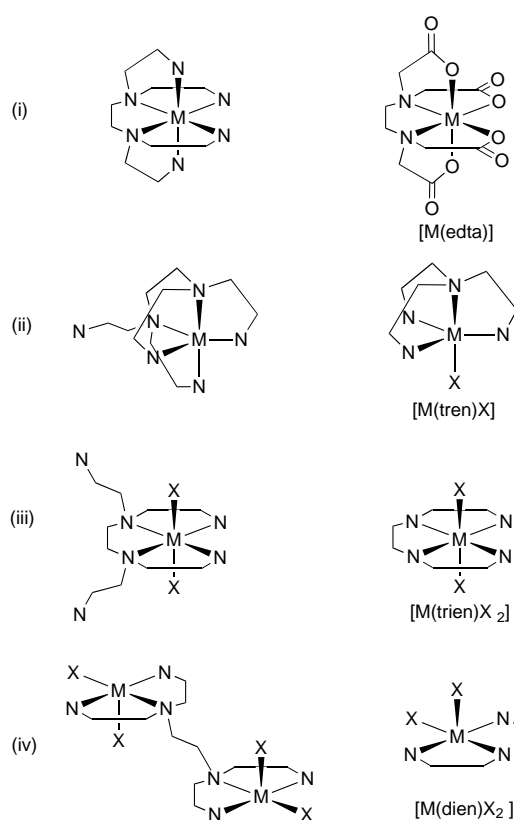
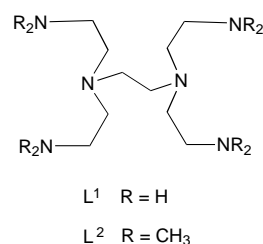


Fig. 1 Potential bonding modes of ligands based on L^1



Experimental

Syntheses

N,N,N',N'-Tetrakis(2-aminoethyl)ethane-1,2-diamine hexahydrobromide ($L^1 \cdot 6HBr$) was synthesized from an optimised literature procedure (in English)¹¹ based on the original preparation (in German).¹ NMR (D_2O): 1H , δ 3.40 (m); ^{13}C , δ 37.7

† Non-SI unit employed: $G = 10^{-4} T$.

(CH₂CH₂NH₂), 51.7 (NCH₂CH₂N) and 52.4 (CH₂CH₂NH₂). Protonation constants (pK_a) 10.5, 9.8, 9.2, 8.4 and 2.6 (lit.,⁷ 10.2, 9.7, 9.1, 8.6 and ≈1.4).

[N,N,N',N'-Tris(2-aminoethyl)-N'-(2-ammonioethyl)ethane-1,2-diamine]copper(II) perchlorate, [Cu(HL¹)](ClO₄)₃. A solution of Cu(NO₃)₂·3H₂O (1.35 g), L¹·6HBr (2.0 g) and NaOH (0.89 g) in water (150 cm³) was stirred at 40 °C for 1 h. The resulting blue solution was filtered and sorbed onto a Sephadex C-25 cation-exchange resin (Na⁺ form). The product eluted from the column with 0.5 mol dm⁻³ NaClO₄ solution and concentration of this solution to ca. 50 cm³ produced blue crystals suitable for X-ray work, which were filtered off, washed with EtOH and air dried (0.68 g). Further crops were obtained from the filtrate (Found: C, 19.8; H, 4.9; N, 13.8. Calc. for C₁₀H₂₉Cl₃CuN₆O₁₂: C, 20.2; H, 4.9; N, 14.1%). Protonation constant (pK_a) 8.3 (lit.,⁷ 8.2).

N,N,N',N'-Tetrakis(2-dimethylaminoethyl)ethane-1,2-diamine, L². A solution of L¹·6HBr (5.0 g) in water (20 cm³) was cooled in ice then NaOH (1.7 g) was added with stirring. Formic acid (70 cm³) was added cautiously followed by formaldehyde solution (60 cm³, 37%) and the mixture was refluxed for 2 d. The solution was evaporated to an oil on a rotary evaporator and treated with NaOH solution (100 cm³, 5 mol dm⁻³). After cooling to room temperature the mixture was extracted with CH₂Cl₂ (5 × 50 cm³). The extracts were combined, dried over Na₂SO₄ then evaporated to give an oil (2.7 g). NMR (CDCl₃): ¹H, δ 2.24 (s, CH₃), ≈2.4 (m, CH₂) and ≈2.6 (m, CH₂); ¹³C, δ 46.0, 53.2, 53.4 and 57.6. Protonation constants (pK_a) 9.5, 9.3, 8.5, 8.2, 7.3 and 2.2.

Aquahydroxo-μ-[N,N,N',N'-tetrakis(2-dimethylaminoethyl)ethane-1,2-diamine]dicopper(II) perchlorate dihydrate, [(H₂O)Cu(L²)Cu(OH)](ClO₄)₃·2H₂O. A solution of L² (1.0 g) and CuCl₂·2H₂O (0.50 g) in water (100 cm³) was stirred at room temperature for 30 min. The mixture was filtered and sorbed onto a Sephadex C-25 cation-exchange column. A minor blue-green band eluted first with 0.5 mol dm⁻³ NaClO₄ as the eluent and was discarded. The desired product eluted as a blue-green band and precipitated as a dark blue powder on concentration to ca. 50 cm³. Crystals suitable for X-ray work were obtained from later crops (Found: C, 25.2; H, 6.0; N, 9.6. Calc. for C₁₈H₅₁Cl₃Cu₂N₆O₁₆: C, 25.7; H, 6.1; N, 10.0%).

Physical methods

Solution UV/VIS spectra were measured on a Perkin-Elmer Lambda 12 spectrophotometer. Cyclic voltammetry was performed with a BAS 100B/W analyser employing a glassy carbon working electrode, an Ag–AgCl reference electrode and a platinum auxiliary electrode. Direct current normal and differential pulse polarography employed an EG&G PARC model 303 dropping mercury electrode. All solutions for electrochemistry were ca. 5 × 10⁻³ mol dm⁻³ in analyte and 0.1 mol dm⁻³ in NaClO₄, and were purged with N₂ before measurement. The stoichiometry of each electron-transfer process was established by wave-height comparisons with known one-electron redox processes. Potentiometric titrations of acidified (HClO₄) aqueous solutions (0.1 mol dm⁻³ NEt₄ClO₄) of ligand or complex were carried out at 298 K with a Metrohm 665 Dosimat and an Orion model 720A pH meter, using NEt₄OH as the base. Data were analysed with the program TITFIT.¹² Electron paramagnetic resonance spectra were measured on a Bruker ER200 D spectrometer as frozen 10⁻³ mol dm⁻³ solutions [dmf–water, (1:2), 77 K]. Spin Hamiltonian parameters were obtained by spectral simulation using EPR50F¹³ for mononuclear complexes and DISSIM¹⁴ for dinuclear complexes. Angular overlap model calculations were performed with the program CAMMAG.¹⁵

Crystallography

Cell constants were determined by a least-squares fit to the setting parameters of 25 independent reflections measured on an Enraf-Nonius CAD4 four-circle diffractometer employing graphite-monochromated Mo-Kα radiation (λ 0.710 73 Å) and operating in the ω–2θ scan mode. Data reduction and empirical absorption corrections (ψ scans) were performed with the XTAL¹⁶ package.

Structure solutions. Structures were solved by heavy-atom methods with SHELXS 86¹⁷ and refined by full-matrix least-squares analysis with SHELXL 93.¹⁸ All non-H atoms were refined with anisotropic thermal parameters except disordered O atoms. The structure of [(H₂O)Cu(L²)Cu(OH)](ClO₄)₃·2H₂O exhibited rather severe disorder in the perchlorate anions in addition to the positions of the aqua and hydroxide ligands. These were refined with partial occupancies and isotropic thermal parameters. Alkyl and amine H atoms were included at estimated positions whereas aqua and hydroxo H atoms were first located from difference maps then restrained in a similar manner to that employed for all alkyl H atoms. Non-coordinated water H atoms were not modelled. Selected bond lengths and angles are presented in Tables 1 and 2, and the atomic nomenclature is defined in Figs. 2 and 3 drawn with PLATON.¹⁹

Crystal data. [Cu(HL¹)](ClO₄)₃, C₁₀H₂₉Cl₃CuN₆O₁₂, *M* = 595.3, monoclinic, space group *P*2₁/*n*, *a* = 11.323(2), *b* = 15.544(2), *c* = 12.690(6) Å, β = 93.31(1)°, *U* = 2230(1) Å³, *D*_c(*Z* = 4) = 1.773 g cm⁻³, μ(Mo-Kα) = 14.09 cm⁻¹, *F*(000) = 1228, *T* = 293 K. Specimen: blue prism 0.6 × 0.6 × 0.5 mm, *T*_{max,min} 0.997, 0.752; *N* = 3919, *N*_o = 3381 [|*F*_o| > 2σ(|*F*_o|)], 2 < θ < 25°, *hkl* 0 to 13, 0 to 18, -15 to 15. Final *R*1 = 0.046, *wR*2 = 0.124, *w*⁻¹ = σ(*F*_o)² + (0.0649*P*)² + 4.90*P* where *P* = (*F*_o² + 2*F*_c²)/3, number of parameters = 300, goodness of fit = 1.079. Residual extrema ±0.8 e Å⁻³.

[(HO)Cu(L²)Cu(OH₂)](ClO₄)₃·2H₂O: C₁₈H₅₁Cl₃Cu₂N₆O₁₆, *M* = 841.1, monoclinic, space group *C*2/*c*, *a* = 25.738(9), *b* = 8.391(3), *c* = 16.348(8) Å, β = 107.58(3)°, *U* = 3366(2) Å³, *D*_c(*Z* = 4) = 1.660 g cm⁻³, μ(Mo-Kα) = 15.77 cm⁻¹, *F*(000) = 1752, *T* = 293 K. Specimen: blue prism 0.3 × 0.3 × 0.3 mm, *T*_{max,min} 0.998, 0.833; *N* = 2962, *N*_o = 2144 [|*F*_o| > 2σ(|*F*_o|)], 2 < θ < 25°, *hkl* -29 to 29, 0 to 9, 0 to 16. Final *R*1 = 0.095, *wR*2 = 0.238, *w*⁻¹ = σ(*F*_o)² + (0.1822*P*)² + 4.26*P* where *P* = (*F*_o² + 2*F*_c²)/3, number of parameters = 218, goodness of fit = 1.121. Residual extrema ±1.5 e Å⁻³.

CCDC reference number 186/872.

See <http://www.rsc.org/suppdata/dt/1998/1037/> for crystallographic files in.cif format.

Results and Discussion

Synthesis of the tertiary hexaamine L² was accomplished by the well known Eschweiler–Clarke *N*-methylation reaction of the parent amine L¹. The NMR spectrum showed that each terminal amine had been dimethylated. The protonation constants of L² were determined by potentiometric titration. The pK_a values (see Experimental section) are somewhat different to those of the parent L¹. Specifically, all six protonation constants were obtained for L², whereas the lowest pK_a for L¹ was too small to be determined potentiometrically. This indicates that the solution conformations of the two pentaprotonated compounds are probably quite different. Intramolecular hydrogen-bonding interactions in [H₄L¹]⁴⁺ and [H₅L¹]⁵⁺ are most likely responsible for the small fifth (2.6) and sixth (<2) protonation constants by comparison with [H₄L²]⁴⁺ (7.3) and [H₅L²]⁵⁺ (2.2). We speculate that the *N*-methyl groups of [H₄L²]⁴⁺ and [H₅L²]⁵⁺ force the two branching tertiary amine lone pairs away from one another thus preventing the sharing of protons between adjacent tertiary amines. This proposition is given support when the binding modes of the two ligands are considered (see below).

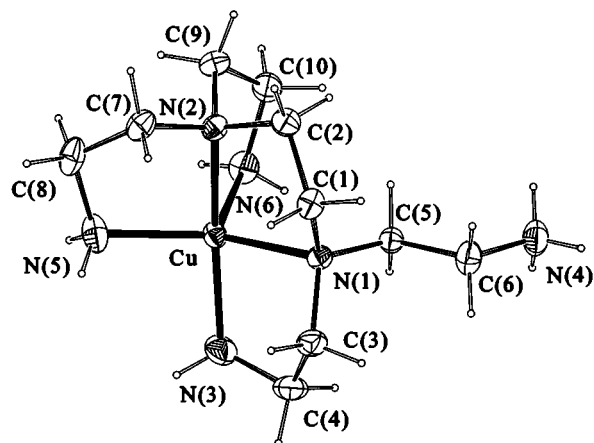


Fig. 2 View of the $[\text{Cu}(\text{HL}^1)]^{3+}$ cation (30% probability ellipsoids shown)

Table 1 Selected cation bond lengths (Å) and angles (°) for $[\text{Cu}(\text{HL}^1)][\text{ClO}_4]_3$

Cu–N(3)	2.000(4)	Cu–N(1)	2.103(3)
Cu–N(2)	2.023(3)	Cu–N(6)	2.147(3)
Cu–N(5)	2.056(4)		
N(3)–Cu–N(2)	166.6(2)	N(5)–Cu–N(1)	138.65(14)
N(3)–Cu–N(5)	95.8(2)	N(3)–Cu–N(6)	107.5(2)
N(2)–Cu–N(5)	85.1(2)	N(2)–Cu–N(6)	84.55(13)
N(3)–Cu–N(1)	84.74(14)	N(5)–Cu–N(6)	110.5(2)
N(2)–Cu–N(1)	85.76(12)	N(1)–Cu–N(6)	108.61(13)

Complexation of both hexamines L^1 and L^2 with Cu^{II} was straightforward and column chromatography indicated that only one species resulted from each reaction. The lability of Cu^{II} facilitated each reaction and one can reasonably assume that the single species observed during chromatography, and upon crystallisation, were the most stable complexes. Micro-analysis indicated that the complex of L^1 possessed a tripositive charge, implying that one of the amines had been protonated, and so was not co-ordinated. The pK_a for this process was found to be 8.3, which compares well with the value originally reported⁷ [pK_a 8.16(2)] in the potentiometric titration of Cu^{II} with L^1 under similar conditions.

The crystal structure of $[\text{Cu}(\text{HL}^1)][\text{ClO}_4]_3$ found the complex cation and three anions all situated on general positions. A view of the cation appears in Fig. 2 showing pentadentate co-ordination of the ligand. The co-ordination geometry (Table 1) most closely resembles a distorted trigonal bipyramid, where the pseudo-three-fold axis is aligned with N(2)–Cu–N(3) [166.6(2)°]. The equatorial N–Cu–N angles are all distorted by more than 10° from an ideal trigonal-planar array, with the N(1)–Cu–N(5) angle being most obtuse [138.7(1)°]. The geometry is distorted towards a square pyramid along the familiar Berry pseudo-rotation coordinate, where the Cu–N(6) bond represents the principal axis of the square pyramid. There are no significant cation–anion interactions. The axial Cu–N bond lengths [2.000(4), 2.023(3) Å] are somewhat shorter than the three equatorial co-ordinate bonds [2.056(4), 2.103(3) and 2.147(3) Å]. This distortion is not related to the type of N-donor (primary or tertiary), but rather is a consequence of the type of co-ordination geometry where a slight axial compression of the trigonal bipyramid is often found. The structure may be compared with that of $[\text{Cu}(\text{tren})(\text{NH}_3)][\text{ClO}_4]_2$ where an almost perfect trigonal-bipyramidal co-ordination geometry was found.²⁰ In that structure the axial Cu–N bond lengths involving the tertiary amine and the ammine ligand were also significantly shorter than those to the three crystallographically equivalent, equatorial primary amines.

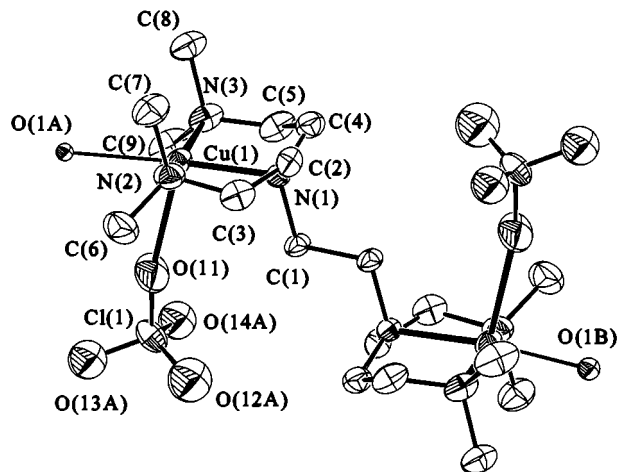


Fig. 3 View of the $[(\text{HO})\text{Cu}(\text{L}^2)\text{Cu}(\text{OH}_2)]^{3+}$ cation (30% probability ellipsoids shown, H atoms omitted for clarity)

Table 2 Selected bond lengths (Å) and angles (°) for $[(\text{HO})\text{Cu}(\text{L}^2)\text{Cu}(\text{OH}_2)][\text{ClO}_4]_3 \cdot 2\text{H}_2\text{O}$

Cu(1)–N(1)	2.037(5)	Cu(1)–O(1B)	2.114(9)
Cu(1)–N(2)	2.044(7)	Cu(1)–O(1A)	2.287(7)
Cu(1)–N(3)	2.056(7)	Cu(1)–O(11)	2.408(8)
N(1)–Cu(1)–N(2)	85.9(3)	N(2)–Cu(1)–O(1A)	86.8(3)
N(1)–Cu(1)–N(3)	85.2(2)	N(3)–Cu(1)–O(1A)	102.3(3)
N(2)–Cu(1)–N(3)	159.1(3)	N(1)–Cu(1)–O(11)	98.1(2)
N(1)–Cu(1)–O(1B)	172.6(3)	N(2)–Cu(1)–O(11)	99.5(3)
N(2)–Cu(1)–O(1B)	98.7(3)	N(3)–Cu(1)–O(11)	100.4(3)
N(3)–Cu(1)–O(1B)	88.6(3)	O(1B)–Cu(1)–O(11)	86.8(3)
N(1)–Cu(1)–O(1A)	172.5(3)	O(1A)–Cu(1)–O(11)	81.4(3)

The analytical results for the copper(II) complex of L^2 were indicative of a more complicated formula. A 2:1 metal:ligand complex cation was found with the formula $[(\text{H}_2\text{O})\text{Cu}(\text{L}^2)\text{Cu}(\text{OH})][\text{ClO}_4]_3 \cdot 2\text{H}_2\text{O}$. The cation was situated on a centre of symmetry, one perchlorate anion was located on a two-fold axis and the remaining molecules occupied general positions. The symmetry of the complex cation resulted in positions of the hydroxide and aqua ligands (on the two crystallographically equivalent metal centres) being disordered. Two discrete positions were located for the aqua and hydroxo O atoms, and these were both refined with 50% occupancies. The Cu–OH bond length is ≈ 0.17 Å shorter than the Cu–OH₂ bond length. Perchlorate anions bind weakly to each metal ion resulting in distorted square-pyramidal $\text{Cu}^{\text{II}}\text{N}_3\text{O}_2$ co-ordination geometries (Fig. 3). There are no significant differences between the three meridional Cu–N bond lengths (Table 2), but the Cu–O bond to the perchlorate ligand is significantly longer than the bonds involving the aqua and hydroxide ligands. The internuclear $\text{Cu} \cdots \text{Cu}$ separation is 7.191(3) Å and the two CuN_3O planes are necessarily parallel as a result of the centre of symmetry.

The solution electronic spectra of the two complexes reflect their distinctly different co-ordination environments (Fig. 4). The spectrum of $[\text{Cu}(\text{HL}^1)]^{3+}$ displayed a broad, distorted maximum at 13 600 cm^{-1} (ϵ 220 $\text{dm}^3 \text{mol}^{-1} \text{cm}^{-1}$) featuring prominent shoulders on the higher- and lower-energy sides. Deconvolution of this peak gave three Gaussian bands with maxima at 11 000, 13 000 and 15 200 cm^{-1} and these are also shown. The spectrum is qualitatively similar to that of $[\text{Cu}(\text{tren})(\text{NH}_3)]^{2+}$ which exhibits maxima 11 400 and 15 200 cm^{-1} .²⁰ For trigonal-bipyramidal copper(II) complexes (D_{3h} symmetry) two electronic transitions are expected, $(d_{xy}, d_{x^2-y^2}) \rightarrow d_z$ (lower energy) and $(d_{yz}, d_{zx}) \rightarrow d_z$, but distortions from this ideal symmetry identified in the crystal structure of $[\text{Cu}(\text{HL}^1)]^{3+}$ are sufficient to remove the degeneracy of these states and at least three transitions can be seen. The spectrum of $[\text{Cu}(\text{HL}^1)]^{3+}$ was

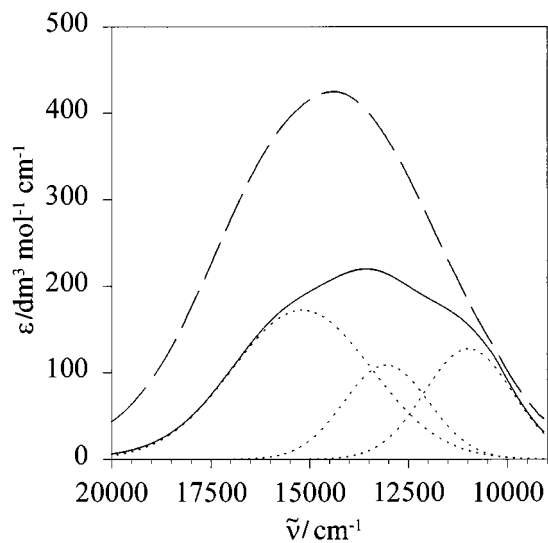


Fig. 4 Aqueous solution electronic spectra of [(HO)Cu(L²)Cu(OH₂)]³⁺ (dashed line) and [Cu(HL¹)]³⁺ (solid line; Gaussian components of band shown as dotted lines)

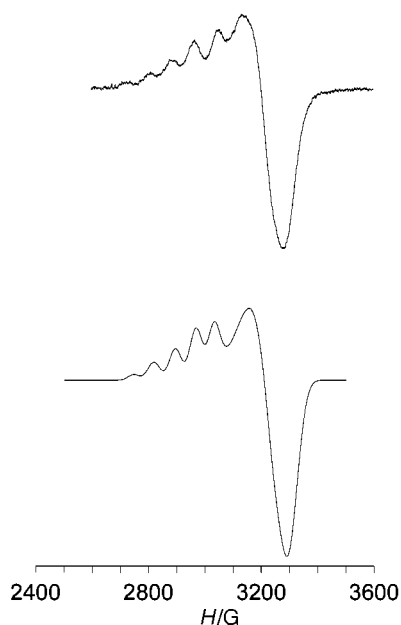


Fig. 5 Experimental (top) and simulated EPR spectra of [(HO)Cu(L²)Cu(OH₂)]³⁺. Solvent: water-dmf (2:1), *T* = 77 K, *ν* = 9.272 GHz

unaffected by the addition of 1 equivalent of base, which indicates that one species was in solution and that the various maxima were not due to different protonated forms of the same complex. The electronic spectrum of [(HO)Cu(L²)Cu(OH₂)]³⁺ exhibited a broad, symmetrical maximum at 14 200 cm⁻¹ (ϵ 425 dm³ mol⁻¹ cm⁻¹ per dimer). This type of spectrum is characteristic of square-pyramidal or tetragonally elongated octahedral copper(II) complexes.

The frozen-solution electron paramagnetic resonance spectra of the two complexes [Cu(HL¹)]³⁺ and [(HO)Cu(L²)Cu(OH₂)]³⁺ were measured. The presence of dipole-dipole coupling between the two proximate copper(II) centres in [(HO)Cu(L²)Cu(OH₂)]³⁺ results in an EPR spectrum (Fig. 5) that is quite unlike that obtained for an isolated mononuclear copper(II) complex. Spin-Hamiltonian parameters were obtained by spectral simulation.¹⁴ These parameters were indicative of square-pyramidal or tetragonally elongated octahedral geometries (*d_{x²-y²}* ground state) with $g_z \gg g_x = g_y$. It is likely that the *z* axes of the two local coordinate systems are approximately aligned with the long axial Cu-O bonds, which are tilted by more than 10° from the normal to their respective CuN₃O

Table 3 Physical properties

	[Cu(HL ¹)] ³⁺	[(H ₂ O)Cu(L ²)Cu(OH)] ³⁺
$\tilde{\nu}_{\max}$ ^a /cm ⁻¹	11 000, 13 000, 15 200 (11 080, 13 700, 14 500)	14 200
g_x ^a	2.264 (2.27)	2.055
g_y ^a	2.140 (2.16)	2.055
g_z ^a	2.025 (2.01)	2.290
A_x /G	131	15
A_y /G	25	15
A_z /G	25	75
$r_{\text{Cu-Cu}}$ ^b /Å	—	7.191(3) (7.2)
ξ ^b /°	—	74 (85)
τ ^b /°	—	0 (0)
η ^b /°	—	0 (0)
E_2 /V vs. Ag-AgCl	-0.59	-0.18

^a Values in parentheses from AOM calculation. ^b Values in parentheses from EPR simulation.

planes. The hyperfine coupling constants are approximately half those found for mononuclear copper(II) analogues, which is a common observation in weakly coupled dinuclear systems such as these.^{22,23} In addition, the spectral simulation yielded values for the intramolecular Cu...Cu separation and the orientation of the two CuN₃O₂ co-ordination spheres. This information is included in Table 3. The geometric parameters obtained from the simulation are not significantly different from those determined from the crystal structure analysis. It should be mentioned that this need not be the case, as large variations between solution and solid-state geometries of dicopper(II) complexes bearing flexible ligands are quite possible.

The EPR spectrum of [Cu(HL¹)]³⁺ (Fig. 6) was consistent with a distorted trigonal-bipyramidal CuN₅ geometry. Spectral simulation¹³ was necessary in order to extract spin-Hamiltonian parameters (Table 3). In this case, $g_x > g_y > g_z$ and $A_x > A_y \approx A_z$. We have modelled the electronic and EPR spectra with angular overlap model (AOM) calculations using the crystallographically determined CuN₅ coordinates. The optimum AOM parameters obtained from fitting the experimental spectra are: e_{σ} /cm⁻¹ N(1) 4900, N(2) 5500, N(3) 5600, N(4) 4900 and N(5) 4000; ζ (spin-orbit coupling constant) 680 cm⁻¹ and k (orbital reduction factor) 0.8. Effects of π bonding and d-s mixing were neglected. Saturated N-donors can be assumed to participate only in σ bonding, and it has been shown that d-s mixing is a minor effect in both high-symmetry²⁴ and distorted²⁵ five-co-ordinate complexes relative to square-planar complexes. When the uncertainties in the observed electronic maxima (Fig. 4) are considered, the agreement between the calculated and observed energies (± 700 cm⁻¹) and EPR g values (± 0.02) was satisfactory (Table 3). In addition the orientation of the g values with respect to the molecular axes was determined. In this case g_z coincides with the pseudo-three-fold axis of the complex and g_x is almost coincident with the Cu-N(6) bond. This is indicated in Fig. 7, where an orbital energy sequence is also given. The figure indicates that the structure of [Cu(HL¹)]³⁺ lies between a trigonal bipyramid and square pyramid. The actual symmetry of the complex is lower than the C_{2v} point group along which the Berry pseudo-rotation coordinate is defined, but this deviation is not considered

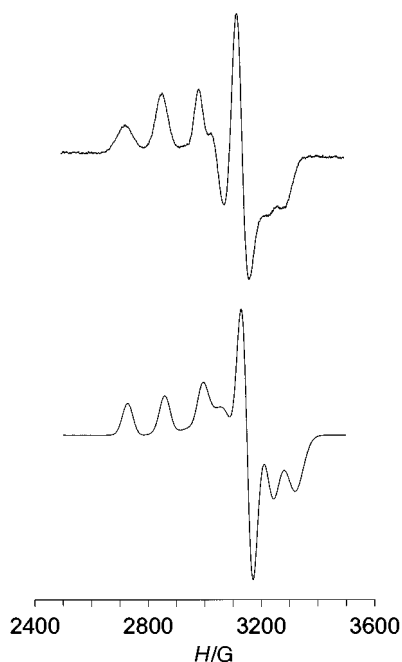


Fig. 6 Experimental (top) and simulated EPR spectra of $[\text{Cu}(\text{HL}^1)]^{3+}$. Details as in Fig. 5

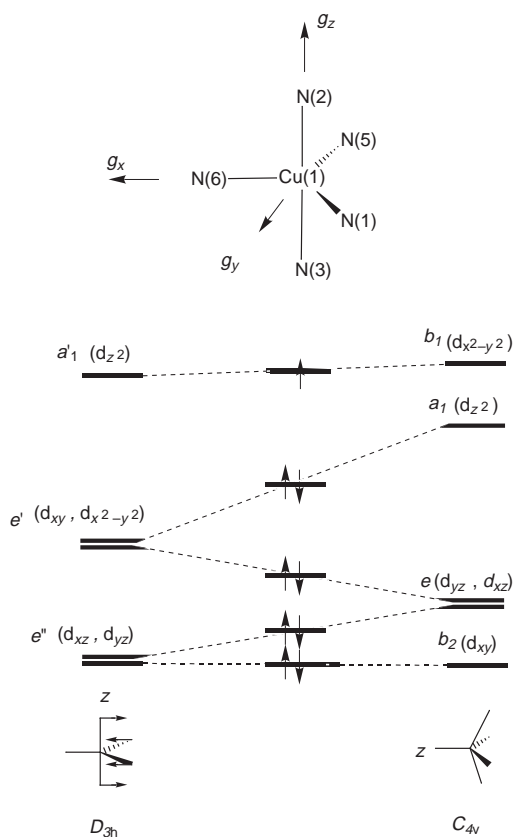


Fig. 7 Qualitative orbital energy diagram for five-co-ordinate copper(II) complexes along a Berry pseudo-rotation coordinate from trigonal bipyramidal (left) to square pyramidal (right) (adapted from ref. 21)

important for the semiquantitative discussion that follows. The unpaired electron occupies an orbital that is strongly antibonding and primarily d_z in character, while the $d_{x^2-y^2}$ orbital lies slightly lower in energy. The calculated energy separation (7350 cm^{-1}) is too small to observe a transition between these states with the available spectrophotometer. The remaining d orbitals at lower energy are effectively non-bonding, with d_{yz} being lowest in energy. The g and A values are comparable with those

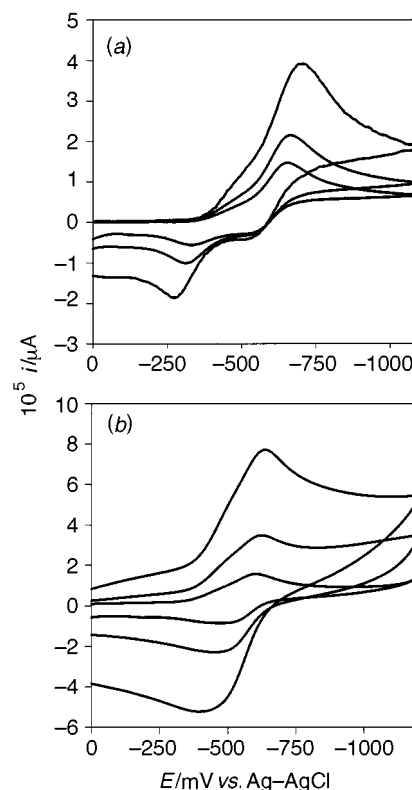


Fig. 8 Cyclic voltammograms of $[\text{Cu}(\text{HL}^1)]^{3+}$: (a) hanging mercury drop working electrode, scan rates 40, 100 and 400 mV s^{-1} ; (b) glassy carbon working electrode, scan rates 20, 100 and 400 mV s^{-1}

obtained from macrocyclic copper(II) complexes exhibiting distorted trigonal-bipyramidal structures.²⁶

Electrochemistry of the complexes $[\text{Cu}(\text{HL}^1)]^{3+}$ and $[(\text{HO})\text{Cu}(\text{L}^2)\text{Cu}(\text{OH}_2)]^{3+}$ was performed in aqueous solution using the techniques of cyclic voltammetry, differential pulse and normal pulse polarography. The $[\text{Cu}(\text{HL}^1)]^{3+}$ ion exhibited a two-electron reduction at $E_1 -0.59 \text{ V vs. Ag-AgCl}$. Cyclic voltammetry employing a hanging mercury drop working electrode [Fig. 8(a)] revealed this redox process to be totally irreversible at all scan rates between 10 and 1000 mV s^{-1} . Cathodic peaks at *ca.* -0.7 vs. Ag-AgCl were accompanied by minor anodic peaks around -0.3 V indicating that the reduced complex undergoes a rapid chemical reaction, probably involving partial dissociation. This anodic process does not correspond to amalgamated Cu as this stripping wave should occur at *ca.* $+0.2 \text{ V vs. Ag-AgCl}$. When a glassy carbon working electrode was used a quasi-reversible Cu^{III} couple resulted [Fig. 8(b)]. The cathodic-anodic peak separation increased markedly with scan rate, which is indicative of a slow electron-transfer rate. It has been found²⁷ that Hg accelerates the rate of disproportionation of copper(I) amines. Therefore, it appears that the loss of a substantial proportion of the putative $\text{Cu}^{\text{I}}\text{-L}^1$ complex at the mercury electrode surface is occurring before reoxidation can occur. This process is slowed sufficiently on the carbon electrode for the observation of a significant anodic wave in the vicinity of the original cathodic wave.

The electrochemistry of $[(\text{HO})\text{Cu}(\text{L}^2)\text{Cu}(\text{OH}_2)]^{3+}$ was more complicated. When a mercury working electrode was used a two-electron redox process was identified at $E_1 -0.18 \text{ V vs. Ag-AgCl}$ corresponding to two simultaneous one-electron reductions of the separate copper(II) centres. This was followed by a broad peak at $-0.49 \text{ V vs. Ag-AgCl}$. This second wave was not present in experiments performed with a glassy carbon electrode, and is thus attributed to strong adsorption of the dicopper(II) complex on the mercury working electrode.²⁸ Adsorption has been found to be a recurring problem in the electrochemistry of tertiary amine copper(II) complexes.²⁹ The redox processes exhibited poor reversibility regardless of the electrode

type indicating that significant rearrangement occurs upon reduction to the monovalent state. This probably comprises a change in co-ordination number (five to four) and geometry (square pyramidal to tetrahedral).

Despite the apparent similarities between the potentially hexadentate amines L^1 and L^2 , their co-ordinating preferences are clearly quite different. The hexamine L^1 has been found to be an effective hexadentate ligand for Co^{III} .^{3,5} In the present case the ligand was found to prefer a pentadentate co-ordination mode when bound to Cu^{II} . Acyclic hexamine complexes of Cu^{II} , e.g. $[Cu(NH_3)_6]^{2+}$ and $[Cu(en)_3]^{2+}$, are typically unstable with respect to hydrolysis, with macrobicyclic cage ligands being required to stabilise the CuN_6 array in aqueous solution.³⁰ A similar result was found in this work where co-ordination of only five of the six amines in $[Cu(HL^1)]^{3+}$ was found. Deprotonation of the free amine does not lead to any significant variation in the visible electronic spectrum, which indicates that the putative $[CuL^1]^{2+}$ is still a five-co-ordinate complex. The predicted structure⁷ of $[Cu(HL^1)]^{3+}$ was actually very close to that ultimately found in this work, but the co-ordination geometry of $[Cu(HL^1)]^{3+}$ was incorrectly assumed to be octahedral (with an aqua ligand completing the co-ordination sphere), rather than the distorted trigonal-bipyramidal structure identified here.

Conclusion

We have found no evidence to suggest that the structure of $[Cu(HL^1)]^{3+}$ is any different in solution compared with that identified in crystal structural analysis. The solution electronic spectrum of $[Cu(HL^1)]^{3+}$ is quite distinct by comparison with those of macrocyclic tetraamine³¹ and macrobicyclic hexamine³⁰ copper(II) complexes, but similar to those of other genuinely five-co-ordinate complexes that have been characterised spectroscopically and structurally in the solid state. Similarly, the structure of the dinuclear $[(HO)Cu(L^2)Cu(OH_2)]^{3+}$ is maintained in solution as shown by EPR spectroscopy. It appears that L^2 is predisposed toward acting as a bridging bis(tridentate) ligand. This is in contrast to the parent L^1 , which can either co-ordinate to one or two metal ions simultaneously depending on the reaction conditions and the preferred co-ordination geometry of the metal. We are currently exploring further aspects of the co-ordination chemistry of this interesting dinucleating ligand.

Acknowledgements

We gratefully acknowledge financial support from the University of Queensland. We also thank Mr. D. Hunter for technical assistance with the EPR measurements. Dr. M. J. Riley is thanked for providing a copy of ref. 25 prior to publication, and for helpful discussions.

References

- 1 W. Gauss, P. Moser and G. Schwarzenbach, *Helv. Chim. Acta*, 1952, **35**, 2359.
- 2 F. Emmenegger, Ph.D. Thesis, ETH, Zürich, 1963.
- 3 K. Hata, M.-K. Doh, K. Kashiwabara and J. Fujita, *Bull. Chem. Soc. Jpn.*, 1981, **54**, 190.
- 4 C. O. Haagensen, *Acta Chem. Scand.*, 1967, **21**, 457.
- 5 A. Muto, F. Marumo and Y. Saito, *Acta Crystallogr., Sect. B*, 1970, **26**, 226.
- 6 K. Sakai, Y. Tanaka and T. Tsubomura, *Acta Crystallogr., Sect. C*, 1996, **52**, 541.
- 7 G. Schwarzenbach and P. Moser, *Helv. Chim. Acta*, 1953, **36**, 581.
- 8 R. Alul, M. B. Cleaver and J.-S. Taylor, *Inorg. Chem.*, 1992, **31**, 3636.
- 9 B. D. Palmer, G. Wickham, D. J. Craik, W. D. McFadyen, L. P. G. Wakelin, B. C. Baguley and W. A. Denney, *Anti-Cancer Drug Des.*, 1992, **7**, 385.
- 10 G. P. Pez, I. L. Mador, J. A. Galle, R. K. Crissey and C. E. Forbes, *J. Am. Chem. Soc.*, 1985, **107**, 4098.
- 11 B. K. Wagon and S. C. Jackels, *Inorg. Chem.*, 1989, **28**, 1923.
- 12 A. D. Zuberbühler and T. A. Kaden, *Talanta*, 1982, **29**, 201.
- 13 R. A. Martinelli, G. R. Hanson, J. S. Thompson, B. Holmquist, J. R. Pilbrow, D. S. Auld and B. L. Vallee, *Biochemistry*, 1989, **28**, 2251.
- 14 J. R. Pilbrow and T. D. Smith, *Coord. Chem. Rev.*, 1974, **13**, 173.
- 15 D. A. Cruse, J. E. Davies, M. Gerloch, J. H. Harding, D. J. Mackey and R. F. McMeeking, CAMMAG, a ligand-field computer program, University of Cambridge, 1991.
- 16 S. R. Hall, H. D. Flack and J. M. Stewart (Editors), *The XTAL 3.2 User's Manual*, Universities of Western Australia, Geneva and Maryland, 1992.
- 17 G. M. Sheldrick, *Acta Crystallogr., Sect. A*, 1990, **46**, 467.
- 18 G. M. Sheldrick, SHELXL 93, Program for Crystal Structure Determination, University of Göttingen, 1993.
- 19 A. L. Spek, *Acta Crystallogr., Sect. A*, 1990, **46**, C34.
- 20 M. Duggan, N. Ray, B. Hathaway, G. Tomlinson, P. Brint and K. Pelin, *J. Chem. Soc., Dalton Trans.*, 1980, 1342.
- 21 A. R. Rossi and R. Hoffmann, *Inorg. Chem.*, 1975, **14**, 365.
- 22 J. F. Boas, R. H. Dunhill, J. R. Pilbrow, R. C. Srivastava and T. D. Smith, *J. Chem. Soc. A*, 1969, 94.
- 23 N. D. Chasteen and R. L. Belford, *Inorg. Chem.*, 1970, **9**, 169.
- 24 L. G. Vanquickenborne and A. Ceulemans, *Inorg. Chim. Acta*, 1981, **20**, 796.
- 25 M. J. Riley, *Inorg. Chim. Acta*, 1997, in the press.
- 26 N. Azuma, Y. Kohno, F. Nemoto, Y. Kajikawa, K. Ishizu, T. Takakuwa, S. Tsuboyama, K. Tsuboyama, K. Kobayashi and T. Sakurai, *Inorg. Chim. Acta*, 1994, **215**, 109.
- 27 D. C. Olson and J. Vasilevskis, *Inorg. Chem.*, 1971, **10**, 463.
- 28 R. H. Wopschall and I. Shain, *Anal. Chem.*, 1967, **39**, 1514.
- 29 P. V. Bernhardt, *J. Am. Chem. Soc.*, 1997, **119**, 771.
- 30 P. V. Bernhardt, R. Bramley, L. M. Engelhardt, J. M. Harrowfield, D. C. R. Hockless, B. R. Korybut-Daszkiewicz, E. R. Krausz, T. Morgan, A. M. Sargeson, B. W. Skelton and A. H. White, *Inorg. Chem.*, 1995, **34**, 3589.
- 31 P. V. Bernhardt, L. A. Jones and P. C. Sharpe, *J. Chem. Soc., Dalton Trans.*, 1997, 1169.

Received 6th October 1997; Paper 7/07209K